Pharmaceutical Research, Vol. 27, No. 5, May 2010 (© 2010)
DOI: 10.1007/s11095-010-0069-y

Research Paper

Influence of Preparation Methods on Solid State Supersaturation of Amorphous Solid Dispersions: A Case Study with Itraconazole and Eudragit E100

Sandrien Janssens,[1] Ann De Zeure,[1] Amrit Paudel,[1] Jan Van Humbeeck,[2] Patrick Rombaut,[1] and Guy Van den Mooter[1,3]

Received October 19, 2009; accepted January 11, 2010; published online March 2, 2010

Purpose. The present study aims to determine the drug / polymer miscibility level as a function of the preparation method for an amorphous solid dispersion model system containing itraconazole and eudragit E100. This value was compared to the theoretical crystalline drug solubility in the amorphous polymer and the miscibility of the amorphous drug in the amorphous polymer.
Methods. The amorphous solid dispersions were prepared via spray drying and film casting in order to evaluate the influence of the solvent drying rate. The experimental miscibility level was estimated using XRPD, MDSC, FT-IR, HPLC and TGA. The solubility and miscibility were estimated using the Flory-Huggins mixing theory and experimental drug in monomer solubility data.
Results. The experimental miscibility level was found to be 27.5% w/w for spray-dried and 15% for film-casted solid dispersions. FT-IR measurements confirmed the absence of saturable interactions like hydrogen bonds, and analysis of the mixed glass transition temperatures suggested low adhesion forces in the amorphous mixture. The solubility analysis rendered a positive FH interaction parameter, a crystalline solubility of approximately 0.012% w/w and an amorphous drug-polymer miscibility of approximately 7.07% w/w.
Conclusion. The solid dispersions are significantly supersaturated with respect to both crystalline solubility and amorphous miscibility demonstrating the influence of manufacturing methodology.

KEY WORDS: amorphous solid dispersions; eudragit E100; itraconazole; miscibility; solid solubility.

INTRODUCTION

Formulation of amorphous drug/polymer blends is becoming an increasingly popular strategy to enhance the absorption of active compounds with dissolution-limited oral bioavailability. The technique relies on dispersion, in the ideal case on the molecular level, of the poorly soluble compound into an amorphous hydrophilic polymer in the solid state. An enhanced dissolution rate is hence obtained by means of particle size reduction and, in the case of molecular dispersion, removal of the crystal lattice. Loss of crystallinity implies that the crystal lattice energy does not have to be overcome for the drug to dissolve. Therefore, this strategy gives rise to spectacular increases in dissolution. Additionally, the carrier can aid dissolution via improved wetting, solubilization and stabilization of the drug in supersaturated solutions (1–4). However, these amorphous drug/polymer formulations are inherently metastable. Indeed, due to preparation processes such as hot stage extrusion or spray drying, where drug/polymer blends are obtained by either fast cooling from a melt or rapid evaporation of a common solvent, the obtained solid is kinetically arrested in a metastable state. This is due to the fact that molecular motions slow down in the solid state and the fact that equilibration can be impeded during preparation. Consequently, the obtained drug/polymer blends are far off the thermodynamic equilibrium. The interplay between thermodynamic driving forces for phase separation and crystallization and kinetic factors, such as molecular mobility, will eventually determine the degree of physical instability (5–7). So far, much research has been performed with respect to drug/polymer compatibility. However, it has been known for a long time already, that properties of amorphous materials are also dependent on their thermal history and, hence, on the mode of preparation (8–10). Therefore, this case study aims to set the limits of both thermodynamic and kinetic miscibility and to demonstrate the influence of kinetics when manufacturing drug/polymer blends. The solid solubility (i.e. the solubility of the crystalline drug in the amorphous polymer) and miscibility (i.e. miscibility of the amorphous drug with the amorphous polymer, amorphous solubility) of itraconazole into eudragit E100 were estimated, and the influence of the solvent evaporation rate on the obtainable degree of supersaturation of itraconazole in the polymer below the glass transition temperature was experimentally assessed by comparing the broadly applied and industrially scalable spray-drying process with a

[1] Laboratorium voor Farmacotechnologie en Biofarmacie, K.U. Leuven, Herestraat 49, bus 921, 3000 Leuven, Belgium.
[2] Department MTM, K.U.Leuven, Leuven, Belgium.
[3] To whom correspondence should be addressed. (e-mail: Guy.Vandenmooter@pharm.kuleuven.be)

film-casting process (11–13). Finally, the obtained results are discussed in comparison with an earlier publication from our group on itraconazole/eudragit E100 solid dispersions prepared by hot melt extrusion (14).

MATERIALS AND METHODS

Materials

Crystalline itraconazole (with a purity of more than 99%) was kindly donated by Johnson and Johnson Pharmaceutical Research and Development (Beerse, Belgium). eudragit® E100 was obtained from Röhm (Darmstadt, Germany). 2-Dimethylaminoethyl methacrylate, methyl methacrylate and butylmethacrylate were kindly donated by Evonik Röhm GmbH (Darmstadt, Germany). All other materials and solvents were of analytical or HPLC grade.

Methods

Spray Drying

Several compositions of itraconazole/eudragit® E100 solid dispersions were prepared (Table I). The spray-drying solutions always contained a total of 5 % (w/v) drug/polymer powder blend in CH_2Cl_2. The solutions were spray dried in a Buchi mini spray dryer B191 (Buchi, Flawil, Switzerland). The aspirator was set at 100% and the pump at 40%. The inlet temperature was set at 45°C, and the air flow was set at 800 L/h. Subsequently, the spray-dried powders were further dried for 1 week at 25°C in a vacuum oven (0.2 bar) and then stored in a desiccator over P_20_5 at 25°C until further analysis.

Film Casting

The samples obtained via film casting were prepared from CH_2Cl_2 solutions with the same compositions as the corresponding spray-dried samples (Table I). The solutions were poured onto a glass plate that was covered with a Teflon® film. A glass funnel with a diameter of 10 cm was then carefully placed over the solution in such a way that there was no contact. A volume of 5 ml was used in order to control the film thickness. To ensure a constant rate of evaporation, the same type of funnel was used for every experiment. The solution was left to dry at room temperature for 60 min. Afterwards, the film was peeled from the glass plate, and liquid nitrogen was poured on the film in order to grind it to a fine powder. These powders were further dried for 1 week at 25°C in a vacuum oven (0.2 bar) and then stored in a desiccator over P_20_5 at 25°C until further analysis.

Differential Scanning Calorimetry (DSC)

Modulated DSC. MDSC analyses were done using a Q2000 Modulated DSC (TA Instruments, Leatherhead, UK) equipped with a refrigerated cooling system. The obtained data were analyzed with the Thermal Analysis software version 4.1D (TA Instruments, Leatherhead, UK). The DSC cell was purged with dry nitrogen (5.5) at a flow rate of 50 ml/min. All measurements were done using crimped aluminum pans (TA Instruments, Leatherhead, UK). The masses of the reference pans and of the sample pans were taken into account when calculating the heat flow. The mass of the samples varied from 4.5 to 7 mg. The modulation parameters were optimized for eudragit® E100. The amplitude was 0.225°C, the period was 25 s and the underlying heating rate was 2°C/min. The samples were heated from 0 to 180°C. The measurements were done in duplicate. The enthalpic response was calibrated with an indium standard, and the temperature scale was calibrated with octadecane, indium and tin. The heat capacity signal was calibrated by comparing the response of a sapphire disk with the equivalent literature value at 57°C. Validation of temperature, enthalpy and heat capacity measurements using the same standard materials showed that the deviation of the experimental from the reference value was <0.5°C for the temperature, < 1 % for the enthalpy and < 1 % for the heat capacity at 57°C. Glass transitions were analyzed in the reversing heat flow and melting, and crystallization transitions were analyzed in the total and the non-reversing heat flow.

Table I. Composition of Samples Prepared by Spray Drying and Film Casting

Spray-dried samples		
Sample	Itraconazole (w/w %)	Eudragit® E100 (w/w %)
SD 2.5%	2.5	97.5
SD 5%	5	95
SD 7.5%	7.5	92.5
SD 10%	10	90
SD 12.5%	12.5	87.5
SD 15%	15	85
SD 17.5%	17.5	82.5
SD 20%	20	80
SD 22.5%	22.5	77.5
SD 25%	25	75
SD 27.5%	27.5	72.5
SD 30%	30	70
SD 35%	35	65
SD 40%	40	60
SD 50%	50	50
SD 60%	60	40
SD 70%	70	30
SD 80%	80	20
SD 100%E100	0	100
Film casted samples		
FC 2.5%	2.5	97.5
FC 5%	5	95
FC 7.5%	7.5	92.5
FC 10%	10	90
FC 12.5%	12.5	87.5
FC 15%	15	85
FC 17.5%	17.5	82.5
FC 20%	20	80
FC 22.5%	22.5	77.5
FC 25%	25	75
FC 27.5%	27.5	72.5
FC 30%	30	70
FC 35%	35	65
FC 40%	40	60
FC 50%	50	50
FC 60%	60	40
FC 100%Itra	100	0
FC 100%E100	0	100

Heat Capacity Determination. Heat capacity measurements were done using a 2920 DSC (TA Instruments, Leatherhead, UK), applying a heating rate of 20°C/min to obtain the difference in heat capacity between the liquid and the crystalline form of itraconazole at a temperature close to the glass transition temperature (67°C). The calorimetric sensitivity, K, was determined from the difference in the baseline heat flow (mW) in the presence and absence of sapphire, ΔY, the heating rate, b (°C/min), the sample mass, M (mg), and the literature values for the Cp of sapphire (J/g.°C), according to the following formula:

$$Cp = K\Delta Y 60/bM \quad (1)$$

in which 60 is a conversion constant (min→s). Consequently, sample heat capacity data were obtained from K, b, and the difference in the baseline heat flow in the presence and absence of sample, ΔY (mW).

X-ray Powder Diffraction (XRPD)

X-ray powder diffraction was performed at room temperature with an X'Pert Pro diffractometer PW 3040/60 (PANalytical, The Netherlands) in Bragg-Brentano geometry and an X'Cellerator PX3015/20 (PANalytical, The Netherlands) detector. The X'Pert Data Collector version 2.2c (PANalytical, The Netherlands) was used for data collection, and the diffractograms were analyzed using the X'Pert Data Viewer version 1.2a (PANalytical, The Netherlands). The system used monochromatic Cu $K_{\alpha 1}$-radiation (λ=1.5418740 Å), which was obtained using a Ni-filter. The radiation passed through a system of soller slits (0.04 rad) and programmable diverging and receiving/anti-scattering slits. The diffraction pattern was measured with a voltage of 45 kV and a current of 40 mA in the region of $2° \leq 2\theta \leq 60°$ in a step scan mode of 0.002° every 20 s. Each sample was back-loaded in a sample holder to minimize possible preferential orientation. The samples that were obtained via film casting were measured in transmission mode. The sample powders were loaded in glass capillaries which were placed in a capillary spinner PW 3063/00. In this setup, a focusing mirror was used, and no divergence slit was present.

Fourier Transform Infrared Spectroscopy (FT-IR)

Samples were prepared using the KBr disk method. Approximately 2 mg of the sample was mixed in an agate mortar with 200 mg dried KBr, and the powder blend was then pressed into a translucent disk. Infrared spectra were obtained on a spectrum RX I FT-IR system (Perkin Elmer, Norwalk, CT, USA). The spectral range was 450 to 4400 cm^{-1} with 16 scans per spectrum and a resolution of 4 cm^{-1}. The spectra were analyzed with the spectrum v2.00 software (Perkin Elmer, Norwalk, CT, USA). The peak positions in the solid dispersion spectra were compared to the peak positions in the spectra of the reference materials made up of glassy itraconazole and eudragit® E100.

Thermogravimetric Analysis (TGA)

An SDT Q600 (TA instruments, Leatherhead, UK) was used to analyze the samples that were obtained by spray drying and by film casting. The instrument was calibrated for weight, temperature and heat flow. The cell was purged with nitrogen at a flow rate of 100 ml/min. Open ceramic sample pans were used for all measurements. The samples were heated from room temperature to 180°C at a heating rate of 2°C/min. The solvent content was determined from the total weight loss at 100°C. The obtained data were analyzed using the Thermal Analysis software version 4.1D (TA instruments, Leatherhead, UK).

Solubility Measurements

An excess of crystalline itraconazole was added to a test tube containing a mixture of three monomers of which eudragit E100 is composed, according to the ratio in the polymer, i.e. 2:1:1 w/w/w 2-dimethylaminoethyl methacrylate, methyl methacrylate, butylmethacrylate. The samples were capped and rotated (Rotator, Snijders Scientific, Tilburg, The Netherlands) for 1 week at room temperature, protected from light. The samples were subsequently filtered with a 0.45µm Teflon filter (Macherey-Nagel, Düren, Germany), properly diluted with methanol (HPLC grade), and the itraconazole content was determined with HPLC (see Section High Performance Liquid Chromatography (HPLC) Analysis), based on a calibration line of standards with known concentration. Experiments were done in triplicate.

Itraconazole Content Determination in the Solid Dispersions

Approximately 50 mg of the solid dispersions was weighed and dissolved in 50 ml methanol. The content of itraconazole was determined with HPLC (see Section High Performance Liquid Chromatography (HPLC) Analysis), based on a calibration line of standards of known concentration. All experiments were done in triplicate.

High Performance Liquid Chromatography (HPLC) Analysis

HPLC analysis was performed using a Merck Hitachi pump l7100, an autosampler (l7200), an ultraviolet (UV) detector (l7400) and an interface (D7000; Merck, Darmstadt, Germany). The column used was a Chromolith performance RP-18e column with a length of 100 mm and a diameter of 4.6 mm (Merck, Darmstadt, Germany). Methanol / tetrabutyl ammonium hydrogen sulphate 0.01 N (70:30; V/V) was used as mobile phase at a flow rate of 1 ml/min. The injection volume was 20 µl; UV detection was used at a wavelength of 260 nm. The itraconazole peak was well separated from the monomer peaks, and its average retention time was 6.4 min.

RESULTS

Amorphicity

XRPD revealed that all of the spray-dried and film-casted samples were X-ray amorphous up to a drug load of 60%. The profiles of the amorphous halos were composition-dependent and represented the sum of the halos of the reference components (Fig. 1).

MDSC revealed recrystallization exotherms and subsequent melting endotherms from a drug load of 20% on for

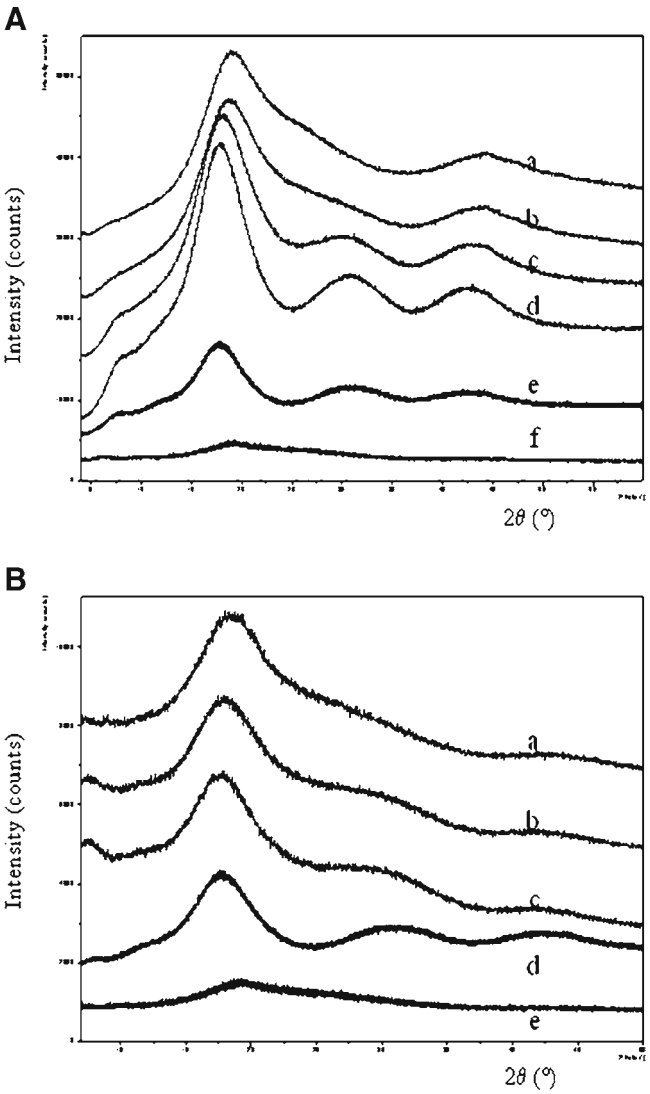

Fig. 1. **A** X-ray diffractograms of spray-dried solid dispersions with, from top to bottom, 80 (*a*), 60 (*b*), 30 (*c*), and 10 (*d*) %w/w itraconazole, eudragit E100 (*e*) and itraconazole (*f*). **B** X-ray diffractograms of film casted solid dispersions with, from top to bottom, 60 (*a*), 30 (*b*), and 10% w/w itraconazole (*c*), eudragit E100 (*d*) and itraconazole (*e*).

spray-dried and from 15% on for film-casted samples. Furthermore, the onset of crystallization was observed at consistently lower temperatures for film-casted samples than for spray-dried samples (Table II). These observations indicate that itraconazole crystallizes more easily upon heating from film-casted samples than from spray-dried samples. A shoulder appeared in the melting peak area from a drug load of 50% or more in the spray-dried samples and 60% or more in the film-casted samples (Fig. 2). This points at the presence of different polymorphic modifications and thus indicates that the preparation method has a distinct influence on the crystallization behavior of the drug in the polymer matrix.

The presence of crystalline material prior to the DSC experiment, i.e. initial crystallinity, was estimated by subtracting the crystallization enthalpy from the melting enthalpy (15). The resulting initial crystallinity estimation was zero for all compositions, indicating that the crystalline material was formed during the DSC run. For compositions where polymorphic modifications were observed, this method could not be applied, since the enthalpy of crystallization differs for different polymorphs.

Drug/Polymer Interactions

Itraconazole and eudragit E100 are both weak bases and hydrogen acceptors, so no specific or directional interactions are to be expected. The absence of specific interactions was confirmed by FT-IR, as the spectra of the solid dispersions simply represented the sum of the reference spectra.

Molecular Level Mixing and Amorphous/Amorphous Phase Separation

As discussed above, the samples were highly amorphous, and no drug/polymer interactions could be observed. Further analysis of the reversing heat flow was very informative regarding the amorphous phase(s) in the samples. Molecular level mixing is recognized by the presence of one single, mixed-phase glass transition. Phase separation can be distinguished by the presence of two consecutive glass transitions and, in the particular case of itraconazole, by the presence of endotherms at 74 and 90°C that are characteristic for its chiral nematic mesophase (16). This mesophase is formed when itraconazole is cooled from the liquid state and is characterized by a first exotherm at 90°C due to the formation of a mesophase, and a second exotherm at 74°C, indicating further restriction of molecular rotation. At 59°C, the mesophase vitrifies. This peculiar phase behavior is convenient when it comes down to identifying a separate glassy itraconazole phase and was considered to be a signature of phase separation. Since the glass transition temperatures of eudragit E100 and itraconazole are very close, 54.3±0.4 and 59.6±0.1°C, respectively, the glass transition temperatures of the amorphous mixtures did not vary much as a function of composition. This also complicated the detection of amorphous/amorphous phase separation, since two consecutive glass transitions might appear as one broad glass transition. The presence of relaxation endotherms in the non-reversing heat flow was therefore selected as a marker for the presence of amorphous phases that had relaxed and facilitated the detection of consecutive glass transitions. In case demixing would have been induced by heating samples in the DSC, the

Table II. Onset of Crystallization Temperatures for Spray-Dried and Film-Casted Samples, $n=2$ and the Error Represents the Range

Drug load (w/w%)	Spray dried (°C)	Film casted (°C)
5	/	/
10	/	/
15	n.o.[a]	110.4±2.7
20	119.6±3.4	112.3±0.9
25	114.0±0.9	109.2±0.7
30	113.4±0.6	105.3±0.3
40	112.8±1.7	104.5±1.3
50	112.4±0.8	104.8±0.1
60	109.7±0.3	99.4±0.1

[a] not observed

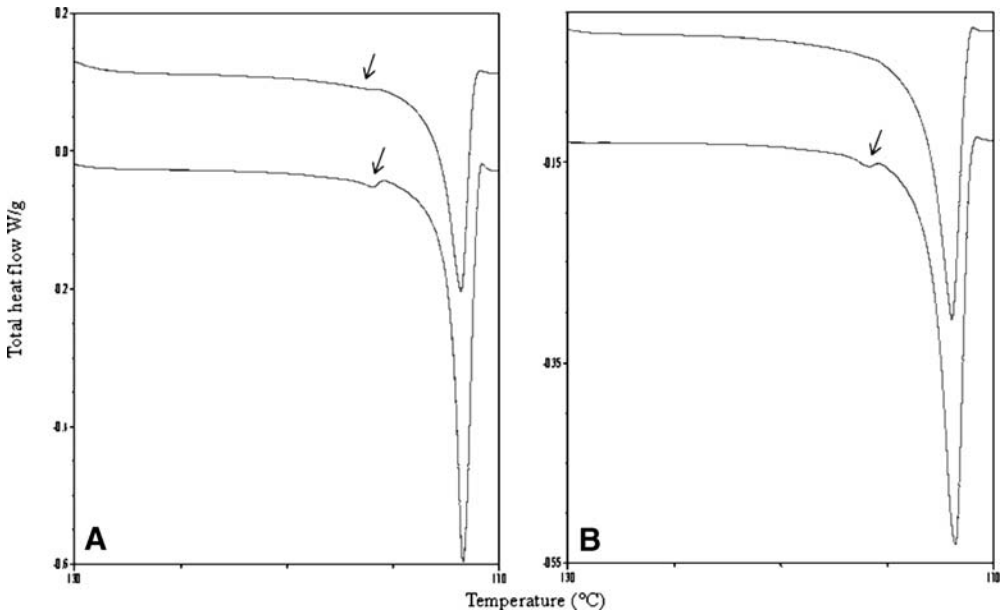

Fig. 2. Total heat flow *versus* temperature for spray-dried solid dispersions **A**, and film-casted solid dispersions **B** with 50 and 60 %w/w itraconazole from top to bottom, the arrows indicate the polymorphic melting endotherms.

newly formed amorphous phase should not have a distinct relaxation endotherm yet. In Table III, an overview of all indicators of phase separation, the presence of mesophase endotherms, two separate glass transitions and two relaxation endotherms, is given for all compositions prepared by spray drying and film casting.

Signs of a glassy chiral nematic mesophase of itraconazole appear at a drug load of 30% w/w for spray-dried samples and at 22.5% w/w for film-casted samples (Fig. 3). For the film-casted samples, the mesophase endotherms are preceded by two glass transitions, the first one representing a polymer-rich phase, and the second one appears at the glass transition temperature of pure glassy itraconazole. The spray-dried samples, on the other hand, do not show the regular mesophase pattern which consists of a glass transition at 59°C followed by two endotherms at 74 and 90°C. The itraconazole glass transition is not clearly resolved from the first polymer-rich glass transition, and only one endotherm is present, slightly below 90°C. Fig. 4 shows how this endotherm increases up to 90°C as the itraconazole drug load increases. The endotherm at 74°C, however, does not appear, even at high drug loads. These features are considered as signs of a disordered mesophase, suggesting interference of the polymer. Up to a drug load of 27.5% w/w, one single glass transition and no signs of a mesophase can be observed; therefore, this drug load denotes the level of miscibility for spray-dried samples.

The film-casted samples already show indications of phase separation at drug loads below 22.5% w/w, before the appearance of the itraconazole glassy mesophase. Indeed, at a drug load of 20%, two separate glass transitions can be observed clearly, and at a drug load of 17.5%, two clearly separated relaxation endotherms can already be identified in the non-reversing heat flow (Fig. 5). Therefore, the level of miscibility for film-casted samples is around 15% w/w.

Analysis of the Mixed Phase Glass Transition

In order to analyse the drug/polymer mixing behavior, all compositions that gave rise to the formation of a single amorphous phase were compared to theoretical predictions of the glass transition temperature for equivalent compositions. Since all samples were dried during 1 week in a vacuum oven, the samples were assumed to be free of residual dichloromethane. Nevertheless, their mass loss at 100°C was determined with thermogravimetric analysis, and the mass loss was attributed to loss of sorbed water. For all samples, weight loss was equal to or below 1.03%. Consequently, the water fraction was estimated from the weight loss. The exact itraconazole fraction in the samples was determined using HPLC, and the polymer fraction was obtained from the difference with the water and itraconazole fractions. Hence, the theoretical glass transition temperatures for ternary drug/polymer/water systems could be obtained from the ternary Gordon-Taylor/Kelly-Bueche equation in combination with the Simha-Boyer rule (17–19):

$$Tg_{mix} = (w_1 Tg_1 + K_1 w_2 Tg_2 + K_2 w_3 Tg_3)/(w_1 + K_1 w_2 + K_2 w_3) \quad (2)$$

Equation 2 is the Gordon-Taylor/Kelly-Bueche equation, in which w is the weight fraction, and Tg is the glass transition temperature (K). The subscripts 1, 2, and 3 represent water, eudragit E100 and itraconazole, respectively. The glass transitions of water, eudragit E100 and itraconazole were −138°C, 54.3±0.4°C and 59.6±0.1°C, respectively. K1 and K2 are constants that were calculated with the Simha-Boyer rule:

$$K \cong (\rho_1 Tg_1)/\rho_2 Tg_2 \quad (3)$$

in which ρ is the density. The subscript 1 represents the amorphous component with the lowest glass transition

Table III. Indicators of Phase Separation for Different Compositions of Spray-Dried (SD) and Film-Casted (FC) Samples, $n=2$

Itraconazole % w/w	Two Tg's	Mesophase	Two enthalpy recovery endotherms
SD 2.5%	–	–	–
SD 5%	–	–	–
SD 7.5%	–	–	–
SD 10%	–	–	–
SD 12.5%	–	–	–
SD 15%	–	–	–
SD 17%	–	–	–
SD 20%	–	–	–
SD 22.5%	–	–	–
SD 25%	–	–	–
SD 27.5%	–	–	–
SD 30%	–	+	–
SD 35%	–	+	–
SD 40%	–	+	–
SD 50%	–	+	–
SD 60%	–	+	–
SD 70%	–	+	–
SD 80%	–	+	–
FC 2.5%	–	–	–
FC 5%	–	–	–
FC 7.5%	–	–	–
FC 10%	–	–	–
FC 12.5%	–	–	–
FC 15%	–	–	–
FC 17.5%	–	–	+
FC 20%	–	–	+
FC 22.5%	+	+	+
FC 25%	+	+	+
FC 27.5%	+	+	+
FC 30%	+	+	+
FC 40%	+	+	+
FC 50%	+	+	+
FC 60%	+	+	+

temperature, and 2 represents the one with the highest glass transition temperature. K1 was calculated from the values for water and eudragit E100; K2 was calculated from the values of eudragit E100 and itraconazole. The densities were 1, 1.09 and 1.27 g/cm^3 for water, eudragit E100 and itraconazole, respectively (14).

For the film-casted samples as well as for the spray-dried samples, it was observed that the experimental glass transition temperatures were all far below the predicted values, even though the plasticizing effect of sorbed water was taken into account (Fig. 6). One of the possible explanations for deviations from Gordon-Taylor/Kelly-Bueche behavior is undetected phase separation. However, this is rather unlikely, since care was taken to only include those compositions that gave rise to a single amorphous phase (one glass transition) and did not show any signs of phase separation, as discussed earlier. Since the glass transition phenomenon is a kinetic event, it also depends on the thermal history of the sample. Indeed, the rate at which a glass is formed from a supercooled liquid will determine at which point the timescale of molecular motions will coincide with the experimental timescale. When this point is reached, the equilibrium super-cooled liquid state will not be attained and the glass is formed (20). Practically, this means that slowly cooled glasses have lower glass transition temperatures than quickly cooled glasses. Similarly, the spray-drying and film-casting process parameters might also influence the position of the glass transition temperature. An interesting paper regarding this effect was recently published by Pinal (21). In this paper, an expression was derived that consists of the regular Couchman-Karasz equation, used to predict the glass transition temperature of amorphous mixtures based on the pure components, and an extra term that describes the entropy of mixing in the mixed glass (22). Deviations towards the values predicted with the Couchman-Karasz equation can be attributed to the amount of configurational entropy that is stored in the glass after cooling from the liquid. Negative deviations indicate that some of the configurational entropy is lost during cooling, which is achieved in a slow cooling process. The expression is applicable on athermal mixtures, meaning that enthalpic contributions do not play a role in the mixing process.

Apart from these effects, the glass transition will deviate from ideal Gordon-Taylor/Kelly-Bueche or Couchman-Karasz behavior if the interactive hetero-molecular forces between drug and polymer are either stronger (positive deviation) or weaker (negative deviation) than the respective interactive homo-molecular forces.

In order to rule out the influence of plasticizing solvents and thermal history on the glass transition temperatures, the spray-dried samples were subjected to a heat-cool-heat sequence, with a maximum temperature after the first heating run of 92°C. This temperature was selected since it is higher than temperatures related to all possible thermal transitions in the amorphous phase and lower than the onset of crystallization. During the first heating run, the residual solvent and moisture are lost, and during the cooling step, the glass is re-formed at a scanning rate of 2°C per min. This scanning rate was also used to determine the glass transitions of the untreated reference components, i.e. itraconazole and eudragit E100. The potential influence of residual plasticizers and the thermal history could thus be investigated. The results of these experiments were compared to theoretical glass transitions that were obtained with the binary Gordon-Taylor/Kelly-Bueche equation for drug/polymer blends in combination with the Simha-Boyer rule and to the values estimated from the Couchman-Karasz equation:

$$\ln Tg_{mix} = \frac{x_1 \Delta C_{p_1} \ln Tg_1 + x_2 \Delta C_{p_2} \ln Tg_2}{x_1 \Delta C_{p_1} + x_2 \Delta C_{p_2}} \qquad (4)$$

where x is the mole fraction concentration, ΔC_p is the difference in the heat capacity of the liquid and the heat capacity of the glass form, and the subscripts 1 and 2 represent eudragit E100 and itraconazole, respectively. The ΔC_ps were 30168, and 301.6 J/mole.K for eudragit E100 and itraconazole, respectively. Again, all the experimental glass transitions were well below the theoretical estimations based on the Couchman-Karasz and the Gordon-Taylor/Kelly-Bueche equation, irrespective of the composition (Fig. 6). Furthermore, no clear trends could be observed between the first heating of the film-casted samples and the first and second heating of the spray-dried samples, regarding the difference between the experimental and estimated values. These results clearly demonstrate that the negative deviations

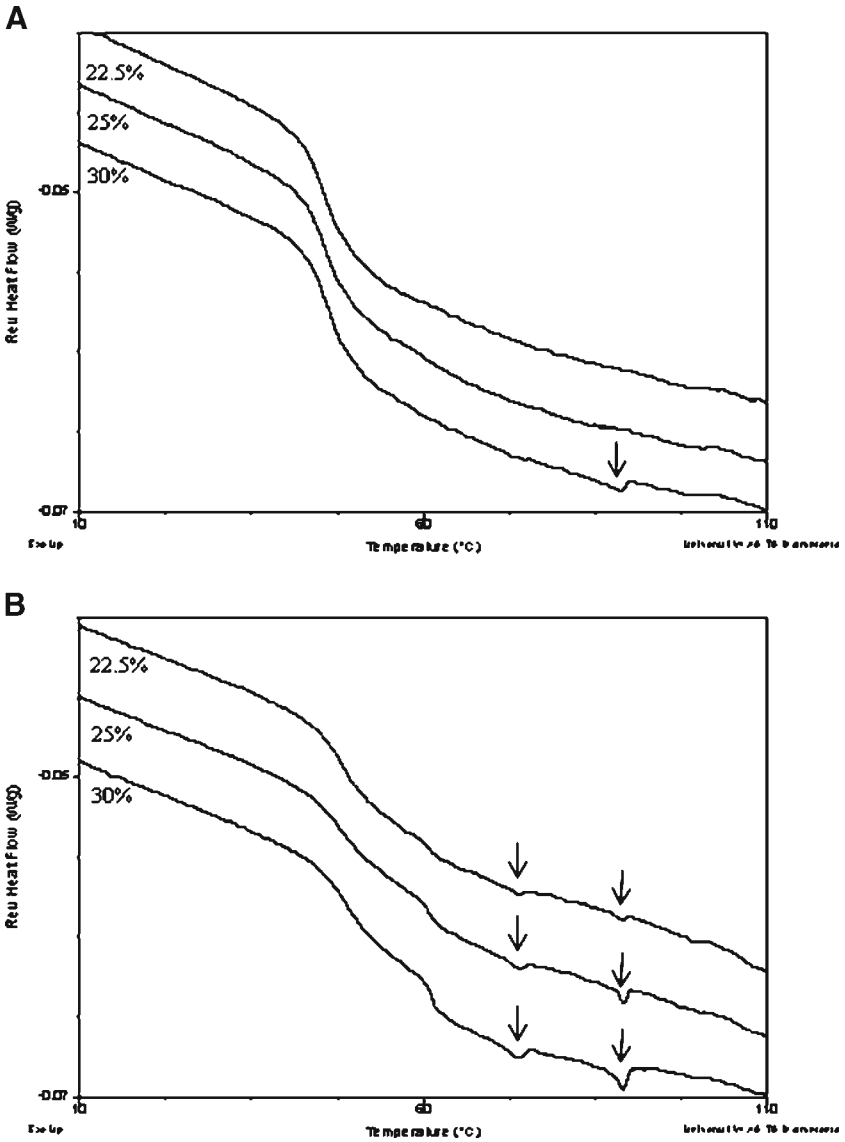

Fig. 3. Reversing heat flow *versus* temperature for spray-dried solid dispersions **A**, and film-casted solid dispersions **B** with 22.5, 25, and 30% w/w itraconazole from top to bottom; the arrows indicate endotherms due to the nematic mesophase of itraconazole.

are not due to differences in the preparation method or the presence of plasticizer, but to the fact that the interactive hetero-molecular forces between itraconazole and eudragit E100 are weaker than the interactive drug/drug or polymer/polymer forces.

Estimation of the Solubility of the Crystalline Drug in the Amorphous Polymer and Miscibility of Amorphous Drug with the Amorphous Polymer

The solid solubility of itraconazole into eudragit E100 was obtained according to methods developed and described by Marsac *et al.* (12,13), using experimental data from the mole fraction solubility of a drug into the monomer which the respective polymer is composed of. The Flory-Huggins (FH) theory of mixing is then used as a theoretical framework. The FH theory defines a hypothetical lattice in space of which each mixture component will occupy a certain amount of positions. The large molar volume difference and the resulting decrease in the entropy of mixing are thereby taken into account for drug-polymer mixtures. Enthalpic contributions between drug and polymer are either derived from solubility or from melting point depression experiments and are described by the FH interaction parameter, χ, which accounts for the enthalpy of mixing in the system in such a way that $\chi=0$ represents athermal mixing, $\chi<0$ represents exothermic and $\chi>0$ represents endothermic mixing. It should be noted that even though in this case χ served as a good measure to point out the importance of enthalpic interactions, it varies with temperature and in some cases also with composition, for example in the case of specific interactions, such as hydrogen bonds. Therefore, the Wertheim lattice thermodynamic perturbation theory, which accounts not only for non-specific interactions but also for specific saturable interactions, might be more suited to describe systems with specific drug/polymer interactions (23,24). However, the absence of

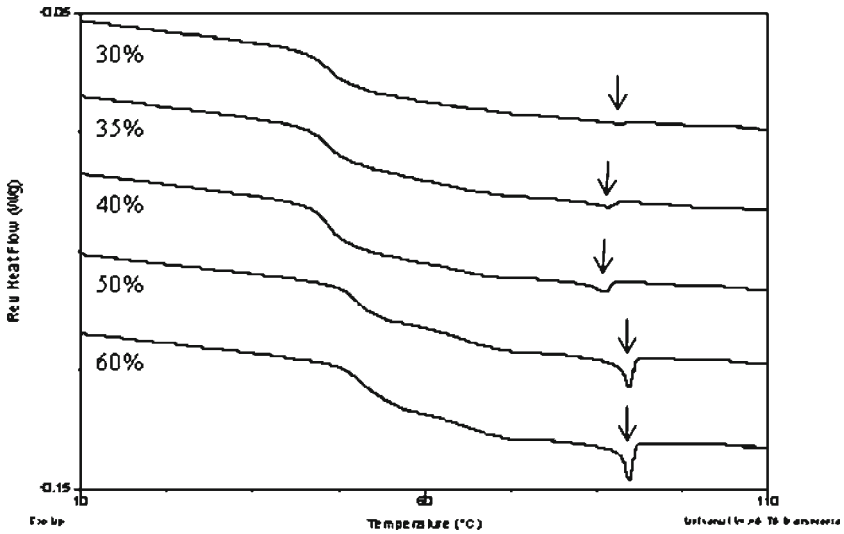

Fig. 4. Reversing heat flow *versus* temperature for spray-dried solid dispersions with 30, 35, 40, 50, and 60% w/w itraconazole from top to bottom; the arrows indicate endotherms due to the nematic mesophase of itraconazole.

directional interactions between itraconazole and eudragit E100 justifies using the FH interaction parameter in this case.

The activity coefficient, γ_{mm}, of itraconazole in a monomer mixture of 2:1:1 w/w/w 2-dimethylaminoethyl methacrylate, methyl methacrylate and butylmethacrylate, the three monomers eudragit E100 is composed of (13,25–27), was obtained by solving the solubility equation of itraconazole in the monomer mixture for ideal solubility, i.e. when γ is 1.

$$\ln \gamma_{mm} x_{drug} = \frac{-\Delta G_{fus}}{RT} = -\frac{\Delta H_{fus}(T_m)}{RT}\left[1 - \frac{T}{T_m}\right] - \frac{1}{RT}\int_{T_m}^{T} \Delta C_p \, dT + \frac{1}{R}\int_{T_m}^{T} \frac{\Delta C_p}{T} dT \quad (5)$$

In this equation, x_{drug} is the mole fraction solubility, ΔG_{fus} is the Gibbs free energy difference between the supercooled liquid and the crystal, T is the absolute temperature (298 K), R is the universal gas constant, T_m is the melting temperature (438.29 K), ΔH_{fus} is the enthalpy of fusion (60.18 kJ/mol) and ΔC_P is the heat capacity difference between the crystal and the supercooled liquid (356.12 J/mol.K). The activity coefficient, γ_{mm}, was then obtained from the ratio of the ideal solubility with the experimental solubility in the monomer mixture. Consequently, the activity coefficient of itraconazole into eudragit E100 was calculated from γ_{mm} by using the Flory-Huggins lattice theory to account for the non-ideal entropy of mixing between a drug and a polymer (13,26–28). It was assumed that the entropy of mixing was ideal for the drug/monomer mixture solution. It was further assumed that the enthalpic contributions to the activity coefficients of itraconazole in the monomer mixture, γ_{mm}, and in the polymer, γ_{E100}, were identical.

$$\ln \gamma_{E100} = \frac{MV_{drug}}{MV_{lattice}}\left[\frac{1}{m_{drug}} \ln \frac{\Phi_{drug}}{x_{drug}} + \left(\frac{1}{m_{drug}} - \frac{1}{m_{E100}}\right)\Phi_{E100}\right] + \ln \gamma_{mm} \quad (6)$$

In this equation, MV is the molecular volume (555.62 cm^3/mol for itraconazole and 149.15 cm^3/mol for the lattice), Φ is the volume fraction, x_{drug} is the experimentally determined mole fraction solubility of itraconazole in the monomer mixture (0.28×10^{-3}), and m is the ratio of the molecular volume of each component to that of the lattice cell. The volume of the lattice cell was defined to be equal to the molecular volume of the monomer. Since there were three monomers, the average value was obtained from the weighed average molecular weight and the experimentally determined density of the mixture. Once γ_{E100} is obtained, the solid solubility of itraconazole can be calculated from the ratio of the ideal mole fraction solubility, 0.016, and γ_{E100}. The Flory-Huggins interaction parameter, χ, can be worked out from equation 7:

$$\ln \gamma_{E100} = \frac{MV_{drug}}{MV_{lattice}}\left[\frac{1}{m_{drug}} \ln \frac{\Phi_{drug}}{x_{drug}} + \left(\frac{1}{m_{drug}} - \frac{1}{m_{E100}}\right)\Phi_{E100} + \chi \Phi_{E100}^2\right] \quad (7)$$

Based on the above-described analysis, the γ_{E100} was determined to be 694.7, the crystalline solubility was estimated to be 0.012% w/w and χ was calculated to be 1.09, demonstrating the extremely low solubility of itraconazole in the amorphous polymer. From the crystalline solubility, we estimated the miscibility of the amorphous drug with the amorphous polymer (or "amorphous solubility") S_a using the following equation (29):

$$S_a = S_c e^{\frac{\Delta S_f}{R} \ln \frac{T_f}{T}} \quad (8)$$

S_c is the crystalline solubility, ΔS_f is entropy of fusion, T_f is the melting point of the drug and T is the absolute temperature (here 298K). S_a was 7.07% w/w. This implies that the solid dispersions are supersaturated with respect to both the crystalline solubility and amorphous-amorphous miscibility and prone to phase separation due to the thermodynamic driving force. Therefore, the system only exists by virtue of kinetic stabilization.

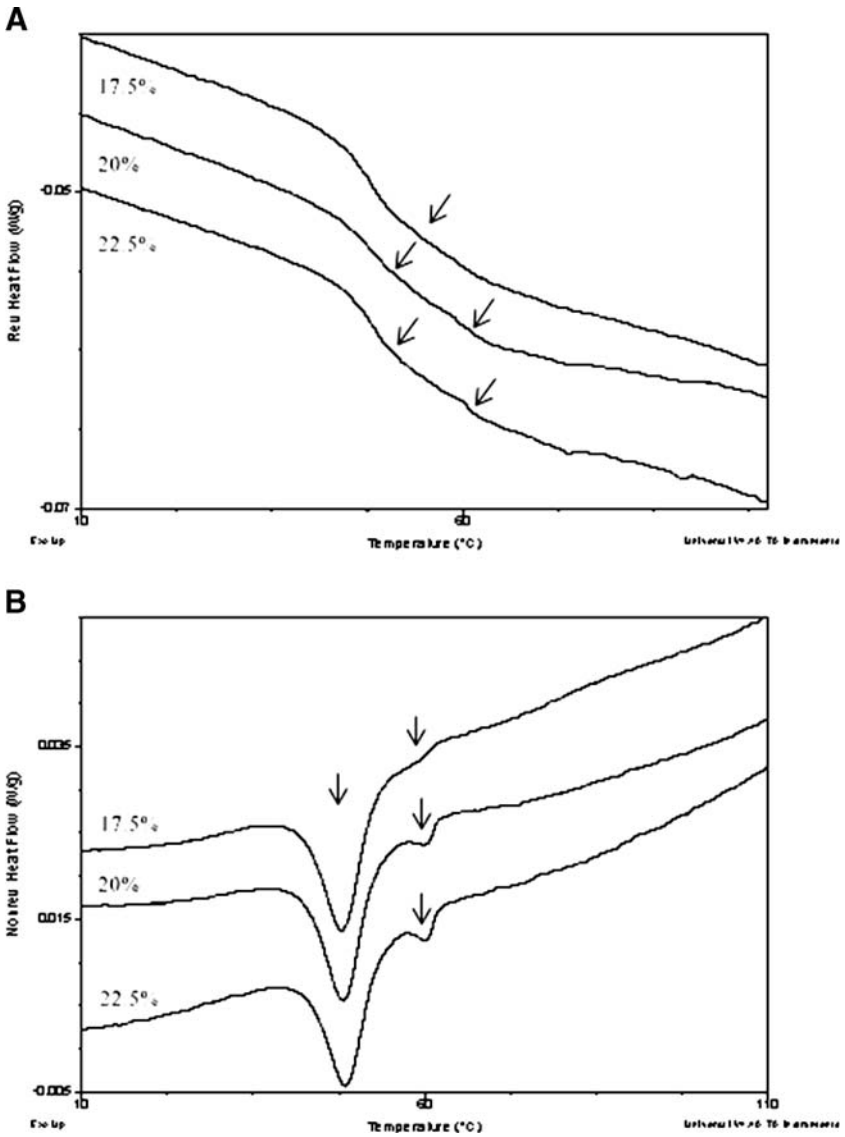

Fig. 5. Reversing heat flow **A** and non-reversing heat flow **B** *versus* temperature for film-casted solid dispersions with 17.5, 20 and 22.5% w/w itraconazole from top to bottom; the arrows in **A** represent glass transitions, the arrows in **B** represent relaxation endotherms.

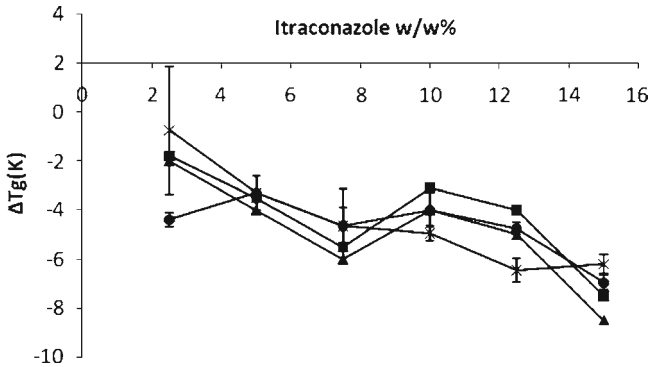

Fig. 6. The difference between the observed and predicted glass transition temperatures (ΔTg) *versus* composition (%w/w) for (●) spray-dried solid dispersions, (x) film-casted solid dispersions, and (■) spray-dried solid dispersions after the heat-cool-heat procedure, using the Gordon-Taylor equation, and (▲) using the Couchman-Karasz equation for the spray-dried solid dispersions after a heat-cool-heat procedure. The bars represent the difference between two measurements.

DISCUSSION

The calculated crystalline solubility as well as the amorphous-amorphous miscibility and the comparison of experimental glass transition temperatures of the mixed amorphous phases indicate that the adhesion forces in itraconazole eudragit E100 glassy mixtures are very low. Indeed, the glass transition temperatures of the single phase amorphous mixtures showed large negative deviations from the predicted values. Furthermore, the estimated crystalline solid solubility, 0.012% w/w, of itraconazole in eudragit E100 was found to be negligible for any realistic or commercially viable pharmaceutical formulation. The miscibility of amorphous itraconazole in eudragit E100 was estimated at 7.07% w/w. These data clearly indicate the difference between amorphous-amorphous miscibility and crystalline solubility. This is not unexpected since miscibility is mainly the result of the balance between adhesion and cohesion forces, while

crystalline solubility also depends on the drug lattice properties. Based on the experimental data, the miscibility limit for itraconazole into eudragit E100 prepared via film casting was found to be 15%, and 27.5% when prepared via spray drying. These data show that generally applied production processes for solid dispersions are able to generate amorphous drug/polymer systems that are significantly supersaturated. Furthermore, the degree of supersaturation can easily be tuned via the production process and process parameters, such as the solvent evaporation rate in this case.

Six *et al.* reported a miscibility limit of ± 15% w/w for itraconazole/eudragit E100 solid dispersions prepared via hot melt extrusion at a temperature above (453 K) and below the itraconazole melting temperature (413 K). This illustrates that in addition to film casting and spray drying, the same degree of supersaturation below Tg can be obtained via heat-based methods.

In this case, it is noteworthy that the glass transition temperature of the polymer is lower than that of the drug. Therefore, the glass transition temperature of the mixture is not increased compared to that of the pure drug, which is generally assumed to be one of the most important mechanisms of kinetic stabilization. However, more detailed studies of the molecular mobility within the drug/polymer system compared to the pure amorphous drug are required to evaluate the antiplasticizing effect in this particular system. Furthermore, the relation between the glass transition temperature and structural relaxation of amorphous materials on one hand and viscosity and diffusion on the other hand is not yet completely understood. Apart from kinetic effects on phase separation, nucleation and crystallization are also associated with kinetic barriers (5). Hence, more fundamental insight regarding specific kinetic barriers should be acquired, now that the importance and potential of kinetic stabilization are acknowledged.

By casting films on Teflon plates covered with a funnel, the evaporation time of dichloromethane could be prolonged significantly to allow the system to equilibrate as much as possible. Still, the miscibility level was substantially above the calculated miscibility limit. For spray-dried samples, the degree of supersaturation was elevated with another 10 %w/w. However, the position of the experimental glass transition temperatures of both film-casted and spray-dried samples did not reveal any information regarding the preparation process. For both data sets, large negative deviations from predicted values were found, but no clear difference could be observed between them. On the other hand, the experimentally obtained miscibility level was significantly different, and this suggests that both samples must have a different physical configuration with corresponding differences in kinetics of phase separation. The data show that the film-casted samples are somewhat more effective in creating a physical configuration that approaches the thermodynamically favored phase separation. So the two methods of preparation produce dispersions of equal composition but different properties over any practical time scale. To further explore the influence of drying kinetics on phase behavior and miscibility, more research is needed. Wulsten *et al.* recently described how levitated single droplet drying can be used to study the spray-drying process (30). The technique relies on stabilization of a droplet in the node of an acoustic wave into a drying chamber with controllable temperature and gas flow. The temperature at the surface of the droplet can be monitored with infra-red thermography, and the droplet dimensions are monitored with a camera. Several stages of drying can thus be identified, and the influence of the drying rate on phase separation and the actual transition from droplet to particle can be evaluated.

CONCLUSION

This study demonstrates the importance of kinetic stabilization with respect to drug-polymer miscibility. The crystalline solubility limit and the Flory-Huggins interaction parameter were determined to be 0.012% w/w and 1.09, respectively. The amorphous drug-polymer miscibility was 7.07% w/w. The experimental miscibility limits of both film-casted and spray-dried itraconazole/eudragit E100 solid dispersions were found to be 15 and 27.5% w/w, respectively, demonstrating the considerable degree of supersaturation below Tg and the importance of the solid dispersion manufacturing methodology.

ACKNOWLEDGEMENTS

The laboratory for pharmaceutical analysis (K.U. Leuven) is acknowledged for the FT-IR measurements, and S.J. acknowledges B.O.F., bijzonder onderzoeksfonds K.U. Leuven, for financial support (PDM grant). This study was supported by a grant from Onderzoeksraad K.U.Leuven (IOF/KP/06/021)

REFERENCES

1. Leuner C, Dressman J. Improving drug solubility for oral delivery using solid dispersions. Eur J Pharm Biopharm. 2000; 50:47–60.
2. Vasconcelos T, Sarmento B, Costa P. Solid dispersions as strategy to improve oral bioavailability of poor water soluble drugs. Drug Disc Today. 2007;12:1068–75.
3. Serajuddin ATM. Solid dispersion of poorly water-soluble drugs: early promises, subsequent problems, and recent breakthroughs. J Pharm Sci. 1999;88:1058–66.
4. Brouwers J, Brewster ME. P. augustijns. Supersaturating drug delivery systems: The answer to solubility limited oral bioavailability? J Pharm Sci. 2009;98:2549–72.
5. Bhugra C, Pikal MJ. Role of thermodynamic, molecular, and kinetic factors in crystallization from the amorphous state. J Pharm Sci. 2007;97:1329–49.
6. Yu L. Amorphous pharmaceutical solids: preparation, characterization and stabilization. Adv Drug Deliv Rev. 2001;48:27–42.
7. Bhattacharya S, Suryanarayanan R. Local mobility in amorphous pharmaceuticals—characterization and implications on stability. J Pharm Sci. 2009;98:2935–53.
8. Savolainen M, Heinz A, Strachan C, Gordon KC, Yliruusi J, Rades T, *et al.* Screening for differences in the amorphous state of indomethacin using multivariate visualization. Eur J Pharm Sci. 2007;30:113–23.
9. Surana R, Pyne A, Suryanarayanan R. Effect of preparation method on physical properties of amorphous trehalose. Pharm Res. 2004;21:1167–76.
10. Willart JF, Descamps M. Solid state amorphization of pharmaceuticals. Mol Pharm. 2008;5:905–20.
11. Peeters J, Neeskens P, Tollenaere JP, Van Remoortere P, Brewster ME. Characterization of the interaction of 2-hydroxypropyl-beta-cyclodextrin with itraconazole at pH 2, 4 and 7. J Pharm Sci. 2002;91:1414–22.

12. Marsac PJ, Shamblin SL, Taylor LS. Theoretical and practical approaches for prediction of drug-polymer miscibility and solubility. Pharm Res. 2006;23:2417–26.
13. Marsac PJ, Li T, Taylor LS. Estimation of drug-polymer miscibility and solubility in amorphous solid dispersions using experimentally determined interaction parameters. Pharm Res. 2009;26:139–51.
14. Six K, Leuner C, Dressman J, Verreck G, Peeters J, Blaton N, *et al*. Thermal properties of hot-stage extrudates of itraconazole and Eudragit E100: phase separation and polymorphism. J Therm Anal Calor. 2002;68:591–601.
15. Van den Mooter G, Wuyts M, Blaton N, Busson R, Grobet P, Augustijns P, *et al*. Physical stabilization of amorphous ketoconazole in solid dispersions with polyvinylpyrrolidone K25. Eur J Pharm Sci. 2001;12:261–9.
16. Six K, Verreck G, Peeters J, Binnemans K, Berghmans H, Augustijns P, *et al*. Investigation of thermal properties of glassy itraconazole: identification of a monotropic mesophase. Thermochim Acta. 2001;376:175–81.
17. Gordon S, Taylor JS. Ideal copolymers and the second-order transitions of synthetic rubbers I. Non-crystalline copolymers. J Appl Chem. 1952;2:493–500.
18. Kelley FN, Bueche F. Viscosity and glass temperature relations for polymer-diluent systems. J Pol Sci. 1961;50:549–56.
19. Simha R, Boyer RF. General relation involving the glass transition temperature and coefficient of expansion of polymers. J Chem Phys. 1962;37:1003–7.
20. Hancock BC, Zografi G. Characteristics and significance of the amorphous state in pharmaceutical systems. J Pharm Sci. 1997;86:1–12.
21. Pinal R. Entropy of mixing and the glass transition of amorphous mixtures. Entropy. 2008;10:207–23.
22. Couchman PR, Karasz FE. A classical thermodynamic discussion of the effect of composition on glass transition temperatures. Macromolecules. 1978;11:117–9.
23. Wertheim MS. Fluids with highly directional attractive forces. I. Statistical thermodynamics. J Stat Physics. 1984;35:19–34.
24. Wertheim MS. Fluids with highly directional attractive forces. II. Thermodynamic perturbation theory and integral equations. J Stat Physics. 1984;35:35–47.
25. Monograph on basic butylated methacrylate copolymer. In European Pharmacopoeia, sixth edition. Strassbourg, France, 2008, pp. 1254.
26. Sandler SI. Chemical & engineering thermodynamics. New York: Whiley; 1999.
27. Yalkowsky SH. Solubility and solubilization in aqueous media. New York: Oxford University Press; 1999. p. 49–80.
28. Flory PJ. Principles of polymer chemistry. Ithaca: Cornell university press; 1953.
29. Luder K, Lindfors L, Westergren J, Nordholm S, Kjellander R. In silico prediction of drug solubility. 3. Free energy of solvation in pure amorphous matter. J Phys Chem. 2007;111:7303–11.
30. Wulsten E, Kiekens F, Van Dycke F, Voorspoels J, Lee G. Levitated single-droplet drying: Case study with itraconazole dried in binary organic solvent mixtures. Int J Pharm. 2009;378:116–21.